

Analysis of Multi-angle Imaging SpectroRadiometer (MISR) aerosol optical depths over greater India during winter 2001–2004

L. Di Girolamo,¹ T. C. Bond,² D. Bramer,¹ D. J. Diner,³ F. Fettingner,¹ R. A. Kahn,³ J. V. Martonchik,³ M. V. Ramana,⁴ V. Ramanathan,⁴ and P. J. Rasch⁵

Received 16 August 2004; revised 2 November 2004; accepted 16 November 2004; published 15 December 2004.

[1] We present the first detailed spatial analysis of a four-year, wintertime visible aerosol optical depth (AOD) climatology from the Multi-angle Imaging SpectroRadiometer (MISR) over greater India. Meteorological fields from the National Centers for Environmental Prediction (NCEP) reanalysis, topographic data, and information related to aerosol source regions are used to explain the spatial patterns in MISR AODs. High AODs are found over much of greater India. The highest AODs are over the northern Indian state of Bihar, where we show that meteorology, topography, and aerosol sources all favor development of a concentrated pool of airborne particles. MISR AODs are validated against five ground-based sites in India and Nepal, revealing similar error characteristics found in other validation studies for the MISR aerosol product. *INDEX TERMS*: 0305 Atmospheric Composition and Structure: Aerosols and particles (0345, 4801); 0345 Atmospheric Composition and Structure: Pollution—urban and regional (0305); 3360 Meteorology and Atmospheric Dynamics: Remote sensing; 3394 Meteorology and Atmospheric Dynamics: Instruments and techniques; 9340 Information Related to Geographic Region: Indian Ocean. **Citation**: Di Girolamo, L., T. C. Bond, D. Bramer, D. J. Diner, F. Fettingner, R. A. Kahn, J. V. Martonchik, M. V. Ramana, V. Ramanathan, and P. J. Rasch (2004), Analysis of Multi-angle Imaging SpectroRadiometer (MISR) aerosol optical depths over greater India during winter 2001–2004, *Geophys. Res. Lett.*, 31, L23115, doi:10.1029/2004GL021273.

1. Introduction

[2] The high aerosol concentrations over India are part of what is now known as the “Atmospheric Brown Cloud” that drapes over a large part of Asia [*Ramanathan and Crutzen*, 2003]. Much has been learned about Indian aerosol properties during the Indian Ocean Experiment [e.g., *Ramanathan et al.*, 2001], but those measurements were confined to oceanic regions. Ground-based measurements of aerosol properties in India [e.g., *Devara*, 1998] provide

crucial long-term measurements, but lack the important spatial coverage that satellites can offer. In this study, we provide the first detailed spatial analysis of the climatological aerosol visible optical depths from the EOS-Terra Multi-angle Imaging SpectroRadiometer (MISR) over the greater Indian landmass during the winter season (December, January, and February, or DJF). We focus on the winter season because the dry Indian monsoon keeps mineral dust concentrations at a minimum, thereby allowing a clearer attribution of our aerosol analysis to other anthropogenic sources.

[3] *Kahn et al.* [2004] provide detailed validation of the MISR aerosol product over a wide range of surface and aerosol conditions. However, validation of satellite aerosol properties tends to be regionally specific as it depends on such factors as the aerosol type and the underlying surface type. Over India, *Kahn et al.* [2004] used only a limited amount of data from the AERONET site in Kanpur [*Holben et al.*, 1998]. Since these data may not be representative of all aerosol and surface conditions over greater India, we extend the MISR validation effort to include ground-based data that we collected over Kathmandu, Nepal and observations from other locations in India reported in the literature. This was undertaken to ensure proper error characteristics of the MISR aerosol optical depths in our analysis.

2. AOD Data

[4] MISR data were collected for DJF of 2001–2004. Version 15 of the MISR Level 2 aerosol product was used and the 558 nm regional mean aerosol optical depth (AOD) was examined in this study. The regional mean AOD is reported at 17.6 km resolution using an automated algorithm that analyzes 16×16 patches of 1.1 km resolution, top-of-atmosphere MISR radiances [*Martonchik et al.*, 2002]. *Kahn et al.* [2004] found, over a wide range of surface and aerosol conditions, that about two-thirds of the MISR-retrieved AOD values fall within 0.05 or 20% of the AERONET AOD values, whichever is larger, with more than one-third within 0.03 or 10%. In regions of heavy pollution, such as would be expected over parts of India, that study found that MISR AOD values were systematically lower than AERONET by ~ 0.1 .

[5] We extend the MISR aerosol validation effort by incorporating data collected at several sites across India and Nepal. Because there were no coordinated efforts between the ground data collection and the MISR overpasses, data sampling was sparse. For example, using the AERONET site in Kanpur, *Kahn et al.* [2004] retrieved only three valid near-spatial-temporal-coincident MISR-

¹Department of Atmospheric Sciences, University of Illinois at Urbana-Champaign, Urbana, Illinois, USA.

²Department of Civil and Environmental Engineering, University of Illinois at Urbana-Champaign, Urbana, Illinois, USA.

³Jet Propulsion Laboratory, California Institute of Technology, Pasadena, California, USA.

⁴Center for Atmospheric Sciences, Scripps Institution of Oceanography, La Jolla, California, USA.

⁵Climate and Global Dynamics Division, National Center for Atmospheric Research, Boulder, Colorado, USA.

Table 1. Information on the Ground-Based AOD Data^a

Location	Lat., Long.	Elevation (m)	Months	Source
Bangalore	12.97°N, 77.58°E	960	D'01, JF'02	<i>Babu et al.</i> [2002]
Kanpur	26.43°N, 80.33°E	142	JFD'01, JFD'02, F'03	AERONET
Kathmandu	27.67°N, 85.31°E	1600	D'02, JF'03	<i>Ramana et al.</i> [2004]
Manora Peak	29.27°N, 79.45°E	1950	JFD'02	<i>Sagar et al.</i> [2004]
Port Blair	11.63°N, 92.71°E	80	F'02	<i>Moorthy et al.</i> [2003]

^aJFD'02 refers to data from the months of January, February, and December of 2002, as an example in interpreting the Months column.

AERONET AOD measurements during the DJF months of their two-year study period. To increase sampling, we compared monthly mean and standard deviation values of AOD between MISR and ground-based measurements originating from five sources summarized in Table 1. The geographic locations of these ground-based sites are depicted in Figure 1. The Kathmandu data were collected using a Microtops Sun photometer with a 500 nm wavelength filter. The details of this data are reported by *Ramana et al.* [2004]. The data used for Manora Peak, Bangalore, and Port Blair were taken directly from the source literature listed in Table 1. The Kanpur data were Level 2.0 Climatology aerosol data retrieved from the AERONET website (<http://aeronet.gsfc.nasa.gov>). Relative to the 17.6 km resolution of the MISR aerosol product, an increase in sampling was obtained by using the average MISR AOD that falls within a 52.8 km × 52.8 km region centered on the location of the ground sites. The exception to this was Port Blair where an 88 km × 88 km region was used because of smaller spatial AOD variability over water.

[6] Ground-based data from all sources report aerosol optical depths at a wavelength of 500 nm. In all but Kathmandu, the ground-based monthly AOD statistics were derived from daily averages of valid optical depth retrievals. The MISR monthly statistics, derived from regional averages of individual overpasses, originated from data collected near 10:30 AM LST due to the sun-synchronous orbit of MISR. In principle, any systematic diurnal cycle in the true AOD will cause a bias in comparing MISR and ground-based AOD. However, any diurnal artifacts in comparing ground-based and MISR AODs would be small since departures from the daily mean are negligible at the late morning acquisition time of the MISR data [*Smirnov et al.*, 2002]. For Kathmandu, where we have collected the data ourselves, monthly AOD statistics were computed from mean AOD measurements collected between 4:40 and 5:40 GMT, which is centered on the mean time MISR is overhead at Kathmandu.

3. Results

[7] Figure 2 shows a scatter plot of MISR 558 nm AOD versus ground-based 500 nm AOD. No correction for the spectral dependence of AOD was performed. However, given the typical angstrom exponent reported for this region [e.g., *Moorthy et al.*, 2003; *Sagar et al.*, 2004], average 558 nm AOD values should be ~10% lower than those at 500 nm. Figure 2 indicates that the MISR AOD are biased low relative to the ground-based AOD over polluted land regions (Kanpur, Bangalore, and Kathmandu). Over these

regions, the mean AOD is 0.48 from ground-based data and 0.31 from MISR data. Accounting for the spectral bias would bring these two values closer together, but the bias would still remain large at ~0.13 AOD or ~25% lower than the ground-based AOD. No significant correlation between the magnitude of this bias and the month were observed. Note that ground-based and MISR AODs exhibit large day-to-day variability as represented by the large standard deviations shown in Figure 2. Over ocean (Port Blair) and pristine land (Manora Peak), the MISR AOD are biased high relative to the ground-based AOD. The results of Figure 2 are consistent with the findings of *Kahn et al.* [2004]. As discussed by *Kahn et al.* [2004], refinements to the MISR calibration and more representative absorbing aerosol properties for polluted regions in the MISR aerosol algorithm are expected to reduce the biases between MISR and ground-based AODs.

[8] Figure 3 shows a four-year, DJF-averaged MISR 558 nm AOD over greater India. Temporal averaging was performed at the original 17.6 km resolution of the MISR aerosol product. No spatial smoothing was performed in order to be true to the MISR data. One artifact in the MISR aerosol product that can be seen in Figure 3 is the discontinuity in AODs across some land-water boundaries (e.g., coastal Gujarat). This is expected given the biases observed in Figure 2 (i.e., a positive bias over water and a

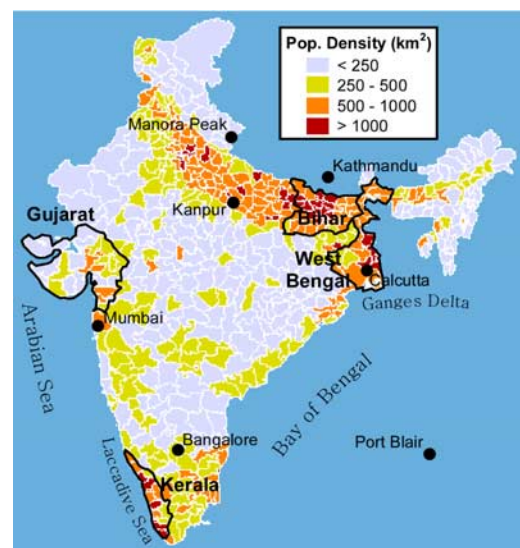


Figure 1. The geographic location of places referred to in the text. These places overlay a population density map of India (by district), based on 2001 census data.

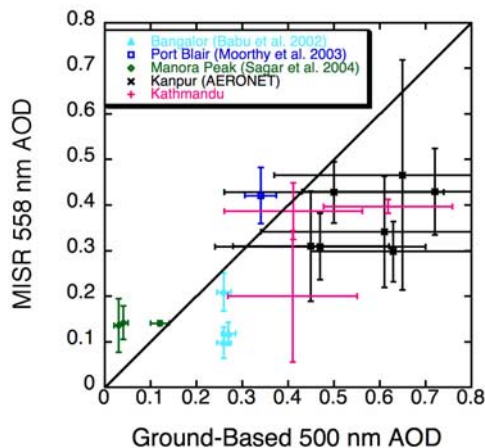


Figure 2. Scatter plot of MISR versus ground-based monthly mean AOD. The error bars represent the standard deviation of AODs used in computing the mean AODs.

negative bias over polluted land). However, some of the largest discontinuities occur in regions where the waters are known to contain extremely large amounts of suspended sediments (e.g., the Ganges delta). Large amounts of suspended sediments invalidate the deep-water assumption used by the MISR aerosol algorithm [Martonchik *et al.*, 2002], resulting in AODs that are biased high. In regions where there are steep gradients in altitude across the land-water boundaries (e.g., the western coast of India (Figure 4)), we would expect part of the discontinuity to be real because of our expectation that lower AODs tend to exist in nature at higher altitudes. In fact, comparing Figure 3 with the topography shown in Figure 4 reveals this correlation between AOD and altitude, which gives further confidence in the MISR AOD product. This correlation alone, however, is not enough to explain the full spatial distribution of AODs in Figure 3; to do so requires topographical, meteorological, and source considerations to be examined in unison. Although there is insufficient space in this letter to discuss all the spatial details in Figure 3, the data and arguments used to discuss several noteworthy regions below can be applied to other regions.

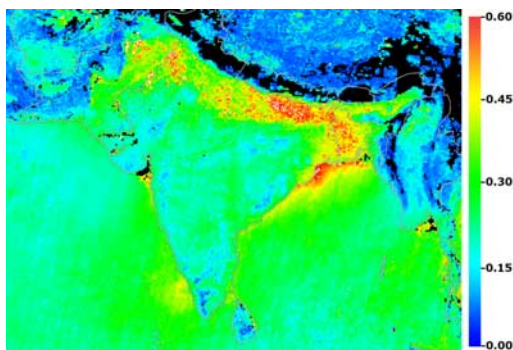


Figure 3. MISR 558 nm AOD averaged over winter (DJF) for 2001 to 2004. Black represents regions where the MISR aerosol algorithm failed to produce any AOD retrieval, due to topographic complexity, persistent cloud, or murky waters. White represent regions of AOD > 0.6.

[9] Meteorological fields were obtained from the NCEP reanalysis (available at <http://www.cdc.noaa.gov>). Although mesoscale flows (e.g., mountain-valley breezes) important in distributing aerosols are likely not captured in this data, the large-scale features that it does capture help to explain some of the spatial variability in AOD. Average meteorological conditions from the NCEP reanalysis over the same period of MISR data used to construct Figure 3 were analyzed. The average surface winds, 850 mb winds, and vertical velocity are overlaid on a topographic map in Figure 4. Precipitation (not shown) over this region during DJF appears not to have any significant impact on the observed AOD distribution, except for the southernmost portion of the Bay of Bengal shown in Figure 3, where the average DJF precipitation reaches around 29 cm/month. This may explain the lower AOD observed in this region compared to its surroundings. Over much of the Indian landmass, precipitation is typically less than 1 cm/month during DJF. Precipitation may affect AOD over the Himalayas in India and Nepal, where it reaches around 10 and 3 cm/month, respectively, during DJF. However, it is difficult to assess its impact in our analysis because large topographic variability precludes valid MISR aerosol retrievals over large portions of the Himalayas, as indicated by the black shaded areas in Figure 3.

[10] For source considerations, we recognize that regional inventories of aerosol emissions carry large uncertainties [Streets *et al.*, 2003; Bond *et al.*, 2004], and a complete discussion of emissions in India is beyond the scope of this paper. However, the population density map shown in Figure 1 assists in understanding the spatial distribution of emissions, and together with Figure 4, it can help explain much of the regional variation observed in Figure 3.

[11] The most striking feature in Figure 3 is the high AODs in the Indo-Gangetic valley. AODs are especially high in the eastern part of this valley, largely within the Indian state of Bihar; hence we will refer to it as “the Bihar pollution pool.” To explain these high AOD values, we note the high (largely rural) population density shown in Figure 1. In India, high population density is often associ-

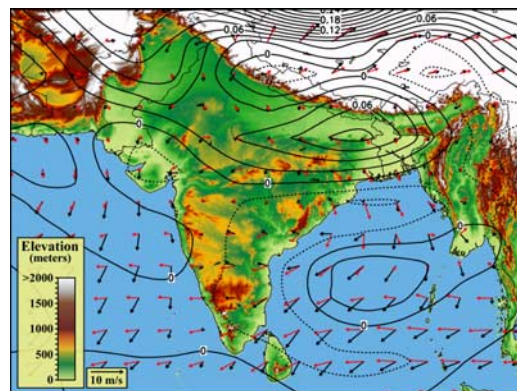


Figure 4. NCEP reanalysis fields overlaying an elevation map of greater India. Black arrows represent surface winds, red arrows represent 850 mb winds, and contour lines represent vertical velocity, where the solid lines represents subsidence and the dashed lines represent ascent. Contour spacing for vertical velocity is 0.02 Pa/s.

ated with large aerosol sources due to fuel consumption [Reddy and Venkataraman, 2002a], including biofuels used for domestic purposes [Reddy and Venkataraman, 2002b]. We expect little biomass burning from agriculture during the DJF growing season. As shown in Figure 4, surface winds are northerly and light, typically 1 to 2 m/s, within the Indo-Gangetic valley. The 850 mb winds are northwesterly, blowing along the valley axis with values of 1 to 4 m/s. Pollutants that blow along the valley from west to east encounter dropping elevations and a narrowing valley floor, both of which would help pool pollutants. Its narrowest width occurs on the eastern side of the state of Bihar, which slows the transport of pollutants from the Bihar pollution pool into West Bengal, Bangladesh, and into the Bay of Bengal. In addition, Figure 4 shows subsiding air over the whole of the Indo-Gangetic valley with a region of maximum subsidence overlapping the Bihar pollution pool. Subsidence acts to inhibit vertical mixing of pollutants to higher altitudes.

[12] Other noteworthy regions include the low AODs in the western Indian state of Gujarat and the high AODs in the Laccadive Sea off the coast of the southwestern Indian state of Kerala (bearing in mind the discontinuities in MISR AODs across land-water boundaries). The low AODs in Gujarat are noteworthy because much of the state resides at low elevation and the state is a large source region of pollutants [Reddy and Venkataraman, 2002a]. However, Figure 4 shows northerly surface winds blowing out to sea and a clear maximum region of ascending air, which increases vertical mixing of pollutants. Figure 1 shows that Kerala is a state with high population density built up along the coast, and high fossil fuel consumption [Reddy and Venkataraman, 2002a]. Pollutants from Kerala and surrounding states are typically blown out to sea from moderately high easterly winds. The high AODs observed over much of the Arabian Sea and Bay of Bengal have been noted before and have been well documented in having a large anthropogenic component, even at distances far from the Indian landmass [e.g., Ramanathan et al., 2001].

4. Discussion

[13] Despite the biases that were characterized in Figure 2 and expected over turbid waters, the spatial distribution of MISR AOD can be explained from the controls of AOD, namely sources, topography, and meteorology, indicating that the spatial aerosol signals observed by MISR are real and not an artifact of the retrieval. Climatological, winter-time MISR AODs are ~ 0.6 for the Bihar pollution pool, where all controls of AOD favor high AOD levels. Although the high levels of pollution in the Indo-Gangetic valley has been known for some time [e.g., Mani et al., 1969], we have not found any literature that discusses, let alone quantifies, the Bihar pollution pool as a large region of high AODs relative to other parts of the Indo-Gangetic valley. We suspect that the Bihar pollution pool must be having a tremendous impact on the local climate and the health of the ~ 100 million people that reside within this pool. Therefore, we would like to call for detailed investigations into the impact of the Bihar pollution pool on local climate and public health.

[14] Our spatial analysis of visible AOD is the most detailed to date over the Indian landmass. The only other study with significant spatial coverage comes from the 4-D data assimilation work of Rasch et al. [2001]. Comparing the spatial distribution of MISR AODs in Figure 3 with the modeled AODs in Plate 1 of Rasch et al. [2001], we find that the most notable differences are that the model results do not place high AODs in the Indo-Gangetic valley. Instead, a band of high AODs stretches over central India from Calcutta to Mumbai. The meteorology reported by Rasch et al. [2001] is similar to the reanalysis data shown in Figure 4, and the model does account for topography. This largely suggests problems with the aerosol source inventory. The inventories used by Rasch et al. [2001] date from the early to mid 1990s. More recent inventories [Reddy and Venkataraman, 2002a, 2002b; Streets et al., 2003; Bond et al., 2004] suggest much more concentrated emissions in the Indo-Gangetic valley and lower emissions over the highlands of southern Bihar. In the earlier study, the location of the peak emission in the highlands of southern Bihar, coupled with the anticyclonic circulation over central India observed in the 850 mb wind field shown in Figure 4, would transport the aerosols across central India instead of pooling them in the valley. This indicates a need for accurate emission inventories for aerosol assimilation models to be successful in predicting the distribution of AODs, where the level of success is measured through its ability to reproduce the observed AOD distributions.

[15] **Acknowledgments.** We thank B. Holben and R. Singh for their effort in establishing and maintaining the AERONET site at Kanpur. The NCEP reanalysis data and the MISR data are distributed by the NOAA-CIRES Climate Diagnostics Center and the NASA Langley Research Center Atmospheric Sciences Data Center, respectively. This work was partially supported by a grant from the National Aeronautics Space Administration's New Investigator Program in Earth Science and through a contract with the Jet Propulsion Laboratory of the California Institute of Technology.

References

- Babu, S. S., S. K. Satheesh, and K. K. Moorthy (2002), Aerosol radiative forcing due to enhanced black carbon at an urban site in India, *Geophys. Res. Lett.*, *29*(18), 1880, doi:10.1029/2002GL015826.
- Bond, T. C., D. G. Streets, K. F. Yarber, S. M. Nelson, J. Woo, and Z. Klimont (2004), A technology-based global inventory of black and organic carbon emissions from combustion, *J. Geophys. Res.*, *109*, D14203, doi:10.1029/2003JD003697.
- Devara, P. C. S. (1998), Remote sensing of atmospheric aerosols from active and passive optical techniques, *Int. J. Remote Sens.*, *19*, 3271–3288.
- Holben, B. N., et al. (1998), AERONET—A federal instrument network and data archive for aerosol characterization, *Remote Sens. Environ.*, *66*, 1–16.
- Kahn, R. A., B. J. Gaitley, J. V. Martonchik, D. J. Diner, and K. A. Crean (2004), MISR global aerosol optical depth validation based on 2 years of coincident AERONET observations, *J. Geophys. Res.*, doi:10.1029/2004JD004706, in press.
- Mani, A., O. Chacko, and S. Hariharan (1969), A study of Angstrom's turbidity parameters from solar radiation measurements in India, *Tellus*, *21*, 829–843.
- Martonchik, J. V., D. J. Diner, K. A. Crean, and M. A. Bull (2002), Regional aerosol retrieval results from MISR, *IEEE Trans. Geosci. Remote Sens.*, *40*, 1520–1531.
- Moorthy, K. K., S. S. Babu, and S. K. Satheesh (2003), Aerosol spectral optical depths over the Bay of Bengal: Role of transport, *Geophys. Res. Lett.*, *30*(5), 1249, doi:10.1029/2002GL016520.
- Ramana, M. V., V. Ramanathan, and I. A. Podgorny (2004), The direct observations of large aerosol radiative forcing in the Himalayan region, *Geophys. Res. Lett.*, *31*, L05111, doi:10.1029/2003GL018824.
- Ramanathan, V., and P. J. Crutzen (2003), New directions: Atmospheric brown clouds, *Atmos. Environ.*, *37*, 4033–4035.

- Ramanathan, V., et al. (2001), Indian Ocean Experiment: An integrated analysis of the climate forcing and effects of the great Indo-Asian haze, *J. Geophys. Res.*, *106*, 28,371–28,398.
- Rasch, P. J., W. D. Collins, and B. E. Eaton (2001), Understanding the Indian Ocean Experiment (INDOEX) aerosol distributions with an aerosol assimilation, *J. Geophys. Res.*, *106*, 7337–7355.
- Reddy, M. S., and C. Venkataraman (2002a), Inventory of aerosol and sulphur dioxide emissions from India: I. Fossil fuel combustion, *Atmos. Environ.*, *36*, 677–697.
- Reddy, M. S., and C. Venkataraman (2002b), Inventory of aerosol and sulphur dioxide emissions from India: II. Biomass combustion, *Atmos. Environ.*, *36*, 699–712.
- Sagar, R., B. Kumar, and U. C. Dumka (2004), Characteristics of aerosol spectral optical depths over Manora Peak: A high-altitude station in the central Himalaya, *J. Geophys. Res.*, *109*, D06207, doi:10.1029/2003JD003954.
- Smirnov, A., B. N. Holben, T. F. Eck, I. Slutsker, B. Chatenet, and R. T. Pinker (2002), Diurnal variability of aerosol optical depth observed at AERONET (Aerosol Robotic Network) sites, *Geophys. Res. Lett.*, *29*(23), 2115, doi:10.1029/2002GL016305.
- Streets, D. G., et al. (2003), An inventory of gaseous and primary aerosol emissions in the year 2000, *J. Geophys. Res.*, *108*(D21), 8809, doi:10.1029/2002JD003093.
-
- T. C. Bond, Department of Civil and Environmental Engineering, University of Illinois at Urbana-Champaign, 205 N. Mathews Ave., Urbana, IL 61801, USA.
- D. Bramer, L. Di Girolamo, and F. Fettingner, Department of Atmospheric Sciences, University of Illinois at Urbana-Champaign, 105 S. Gregory St., Urbana, IL 61801, USA. (larry@atmos.uiuc.edu)
- D. J. Diner, R. A. Kahn, and J. V. Martonchik, Jet Propulsion Laboratory, California Institute of Technology, 4800 Oak Grove Dr., Pasadena, CA 91109, USA.
- M. V. Ramana and V. Ramanathan, Center for Atmospheric Sciences, Scripps Institution of Oceanography, 9500 Gilman Drive, La Jolla, CA 92037, USA.
- P. J. Rasch, Climate and Global Dynamics Division, National Center for Atmospheric Research, P.O. Box 3000, Boulder, CO 80307, USA.